Journal of Biomedical Optics 7(3), 329–340 (July 2002)

Imaging skin pathology with polarized light

Steven L. Jacques
Jessica C. Ramella-Roman
Ken Lee
Oregon Health and Science University
Departments of Dermatology
Electrical and Computer Engineering
Portland, Oregon
and
Providence St. Vincent Medical Center
Oregon Medical Laser Center
Portland, Oregon

Abstract. Linearly polarized light that illuminates skin is backscattered by superficial layers and rapidly depolarized by birefringent collagen fibers. It is possible to distinguish such superficially backscattered light from the total diffusely reflected light that is dominated by light penetrating deeply into the dermis. The method involves acquisition of two images through an analyzing linear polarizer in front of the camera, one image (I_{par}) acquired with the analyzer oriented parallel to the polarization of illumination and one image (I_{per}) acquired with the analyzer oriented perpendicular to the illumination. An image based on the polarization ratio, $\mathrm{Pol}=(I_{par}-I_{per})/(I_{par}+I_{per})$, is created. This paper compares normal light images, represented by I_{per}, and Pol images of various skin pathologies in a pilot clinical study using incoherent visible-spectrum light. Images include pigmented skin sites (freckle, tattoo, pigmented nevi) and unpigmented skin sites [nonpigmented intradermal nevus, neurofibroma, actinic keratosis, malignant basal cell carcinoma, squamous cell carcinoma, vascular abnormality (venous lake), burn scar]. Images of a shadow cast from a razor blade onto a forearm skin site illustrate the behavior of Pol values near the shadow edge. Near the shadow edge, Pol approximately doubles in value because no I_{per} photons are superficially scattered into the shadow-edge pixels by the shadow region while I_{par} photons are directly backscattered from the superficial layer of these pixels. This result suggests that the point spread function in skin for cross-talk between Pol pixels has a half-width-half-max of about 390 μm.
[DOI: 10.1117/1.1484498]

Keywords: polarized light; imaging; skin; biomedical optics.

Paper JBO-TP-I5 received Mar. 18, 2002; revised manuscript received Apr. 2, 2002; accepted for publication Apr. 4, 2002.

1 Introduction

As polarized light propagates through light-scattering media such as biological tissues, microsphere solutions, or an atmosphere with particulates, the polarization status of the light changes. Hence, a medium can be characterized by the degree to which polarized light is altered during propagation. The propagation of polarized light through a biological tissue causes the polarization status of photons to change due to tissue birefringence and tissue scattering. Imaging with polarized light can select light that backscatters from the superficial tissues, in contrast to light that reflects from the air/tissue surface or light that propagates deep into the tissue before eventual escape as diffuse reflectance and whose polarization status has been fully randomized. Hence, images can characterize the superficial region of a tissue which is often the region where cancer develops.

The ability of polarized light to aid imaging of tissues has a long history not fully summarized here. Anderson[1] reported on the dermatologic practice of illuminating with linearly polarized light and observing through a linear polarizer oriented perpendicular to the orientation of the illumination light so as to avoid surface glare. Schmitt et al.[2] reported on the loss of the degrees of linear and circular polarization as linearly and circularly polarized light propagates in light scattering media. Jacques et al.[3] reported on the point-spread function of reflected polarized light in turbid media and proposed the use of polarized light for reflectance video imaging of superficial tissues. Ostermeyer et al.[4] considered a two-scatter model that explained the cross-shaped point-spread function of reflected linearly polarized light in microsphere solutions when observed through a linear polarizing filter. They demonstrated that the point-spread function in skin was minimal which suggested that reflected polarized light imaging in skin would not suffer significant blurring and therefore imaging of superficial skin was feasible. Demos et al.[5] reported on time-resolved measurements of polarized light transport and demonstrated charge coupled device (CCD) imaging with reflected polarized light similar to Ref. 3. Jacques and Lee[6] described polarized light imaging of the superficial layers of skin using the method described in this paper.

Hielscher et al.[7] pursued CCD camera imaging of reflected polarized light in microsphere solutions and reported on how particle size influences the cross-shaped pattern. They also showed that cell solutions could replace microsphere solutions and provide a cross-shaped pattern for analysis. Mourant et al.[8] continued the CCD camera imaging on cell suspensions

Address all correspondence to Steven L. Jacques, Oregon Medical Laser Center, 9205 SW Barnes Rd, Portland, OR 97225. Tel: 503-216-4092; Fax: 503-216-2422; E-mail: sjacques@ece.ogi.edu

1083-3668/2002/$15.00 © 2002 SPIE

and reported on the wavelength dependence of polarized light in solutions of normal and cancerous cells.

Jarry et al.[9] studied the randomization of linearly polarized light as it propagated through tissues and microsphere solutions, observing a surprising persistence of polarization when propagating through liver tissues despite multiple scattering of photons. Sankaran et al.[10] also studied the rates of depolarization. Jacques et al. reported[11] similar findings and expanded the observation to three tissue types, skin liver, and muscle. They proposed a heuristic model that described how the angle of orientation of linearly polarized light diffuses in angle space as the light propagates through tissue, and this diffusion process is characterized by an angular diffusivity, (rad^2/mean free path), that characterizes each tissue type and appears to scale with the birefringence of the tissue (skin $>$muscle$>$liver). Sankaran[12,13] studied the influence of densely packed microsphere solution on the transmitted polarized beam, demonstrating that the behavior of polarized light in tissues is similar to the behavior in densely packed microsphere solutions, a situation that does not conform to the predictions of Mie theory for isolated microspheres. Studinski and Vitkin[14] proposed a method to examine polarized light interaction with tissues in the exact backscattered direction. They found that in the backscattered direction a significant fraction of the incident polarization is preserved, even for highly concentrated media and for biological tissues this confirms theoretical finding of other authors as cited by Brosseau.[15]

Consideration of the wavelength spectrum for backscattered polarized light is a means of characterizing the size of cellular particles such as the nuclei of cells. Backman et al.[16] used polarized light scattering spectroscopy to quantitatively measure epithelial cellular structures *in situ*. Perelman et al.[17] measured nuclear size distribution of mucosal tissue using an optical fiber probe and polarized light. Sokolov et al.[18] reported a simple model that simulated the wavelength dependence of polarized light scattering from monolayers of microspheres and cells.

The use of polarized light with optical coherence tomography (OCT) was introduced by de Boer et al.[19] illustrating the birefringence of collagen in skin and the loss of such birefringence when skin is thermally damaged. Wang et al.[20] introduced Mueller matrix OCT which could create an image based on each of the 16 elements of the Mueller matrix that describes how an optical medium alters the polarization state of incident light as the light transports through the medium. Smith[21] has reported on Mueller matrix imaging and measurements of the diattenuation and retardance of laser light reflected from skin as a function of incident angle and scattered angle.

This paper focuses on the use of polarized light for imaging of the skin. In dermatology, illumination with linearly polarized light and viewing of the skin with an analyzing linear polarizer allows a dermatologist to either emphasize or suppress the glare from the air/skin surface so as to better view the tissue surface or the subsurface tissue structures, respectively, as described by Anderson.[1] Orientation of the analyzer parallel to the orientation of polarization of the illumination light emphasizes the skin surface by accepting photons reflected from the air/skin surface (glare) and rejecting half of the diffusely reflected light (subsurface scattering). Perpendicular orientation of the analyzer suppresses the skin surface and emphasizes the subsurface skin structures by rejecting the surface glare and accepting half of the diffusely reflected light. The diffusely reflected light consists of photons that have penetrated deeply into the skin and have been depolarized by the birefringent dermal collagen fibers. The term ''deep'' here refers to penetration into the reticular dermis perhaps to a depth of 300 μm or more below the skin surface. Such light acts as a back-illumination that returns through the overlying superficial skin layers (papillary dermis and epidermis) to reach the eye. Absorption by hemoglobin in superficial blood vessels attenuates the returning light. Therefore, much of the enhancement by viewing through a perpendicular polarizer is due to better contrast for superficial blood vessels. Demos and Alfano also reported on this use of crossed linear polarizers to enhance imaging of blood vessels.[5]

This paper describes an imaging method introduced by Jacques et al.[10] which differs from both the earlier situations. A glass plate contacts the skin and is optically coupled to the skin by a drop of water or other index matching medium. Illumination by linearly polarized light is delivered from an angle such that glare from the air/glass/skin interfaces is directed away from the viewing camera. The camera only collects light that has entered the skin and been backscattered toward the camera. Image acquisition with an analyzing polarizer oriented parallel to the illumination accepts ''subsurface glare'' due to still polarized light that is scattered in the superficial tissue regions. Acquisition of a second image with the analyzer oriented perpendicular to the illumination accepts primarily deeply scattered photons. Algebraic combination of these two images yields an image that suppresses the diffusely reflected photons that deeply penetrated the skin. The result is an image of subsurface glare which constitutes usually about 5%–10% of the total subsurface reflectance. The image emphasizes the viewing of superficial skin structures that scatter light rather than structures that absorb light. Such images are sensitive to the texture of the superficial skin structures, in particular the papillary and superficial reticular dermis.

In this report, some preliminary clinical images from various skin pathologies are shown. The importance of imaging with a glass plate optically coupled by a drop of water or other index-matching liquid to the skin is illustrated. The point spread function for crosstalk between pixels in a Pol image of skin is demonstrated.

2 Materials and Methods

2.1 Camera System

The camera system is schematically depicted in Figure 1. An incoherent white light source (xenon lamp source, Oriel, Stratford, CT) was passed through a long-pass transmission filter ($>$500 nm wavelength) and a linear polarizer (Ealing Electrooptics, plc., Watford, UK) to yield linearly polarized light. The wavelength of illumination does not strongly influence the depth of imaging which is governed by the rates of depolarization by birefringent tissue structures such as collagen or actin-myosin fibers and depolarization by scattering. Laser light was avoided because laser speckle interfered with the polarization images. The light was collimated by a 20 cm focal length lens and delivered to the skin at an angle of 15°

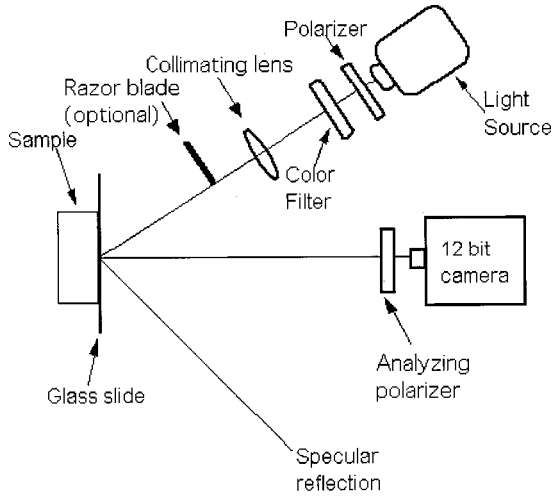

Fig. 1 Schematic of camera system. Collimated white light source is filtered by a bandpass filter and passed through a linear polarizer oriented parallel to source/sample/camera plane. Sample is coupled to glass plate by drop of water. Specular reflectance from air/glass/skin surface is reflected away from the camera. Light that enters the tissue and backscatters toward the camera passes through an analyzing linear polarizer oriented either parallel or perpendicular to the orientation of the source polarization, yielding two images called I_{par} and I_{per}, respectively.

to the normal to the skin surface. The choice of angle is not critical and oblique angles of illumination beside 15° also work. A glass plate contacted the skin and was optically coupled to the skin by a drop of water. Glare from the air/glass/skin interfaces was directed away from the viewing camera. Because polarized light imaging is based on scattering rather than on absorption, there are no problems with the contact pressure of the skin against the glass plate blanching the cutaneous blood vessels. The camera (Princeton Instruments, Trenton, NJ; 16-bit CCD camera) with macro lens (Nikon, Melville, NY; *f* 105 mm, 1:2.8 D) only collected light that had entered the skin and been backscattered toward the camera. For some of the experiments reported here, a razor blade was placed in the illumination beam to cast a shadow on the skin surface. A second analyzing linear polarizer in front of the camera was manually aligned either parallel or perpendicular to the orientation of the polarization of the illumination light which was parallel to the plane defined by the source-skin-camera triangle. Two images were acquired, one called I_{par} when the analyzer was parallel to the illumination and the second called I_{per} when the analyzer was perpendicular to the illumination. The camera integration time for each image was 1 s, although shorter times are possible with stronger illumination. Images were acquired as 600×600 images with 34×34 μm^2 pixels using a library of C programing code and a custom program written with MATLAB™ software to control the camera.

2.2 Signal Processing

The analyzing linear polarizer in front of the camera was oriented parallel to the illumination light (I_0) to acquire an image called I_{par}. The I_{par} image consisted of the superficially reflected light (R_s) plus one half of the deeply penetrating light (R_d). The term ''deeply penetrating'' refers to light penetration into the reticular dermis perhaps to a depth of about 300 μm or more. Any epidermal melanin acted as an absorption filter on the skin surface with a roundtrip in/out transmission of T_{mel}. The I_{par} image is described:

$$I_{par}=I_0T_{mel}(R_s+\tfrac{1}{2}R_d). \quad (1)$$

Then the analyzer was oriented perpendicular to the illumination to acquire an image called I_{per}. The I_{per} image rejected the superficially polarized light but accepted half of the deeply penetrating light. The I_{per} image is described

$$I_{per}=I_0T_{mel}\tfrac{1}{2}R_d\,. \quad (2)$$

The polarization ratio (Pol) was calculated

$$\mathrm{Pol}=\frac{I_{par}-I_{per}}{I_{par}+I_{per}}=\frac{I_0T_{mel}(R_s+\frac{1}{2}R_d)-I_0T_{mel}\frac{1}{2}R_d}{I_0T_{mel}(R_s+\frac{1}{2}R_d)+I_0T_{mel}\frac{1}{2}R_d}=\frac{R_s}{R_s+R_d}. \quad (3)$$

The Pol image was based on the ratio of a numerator that emphasized superficial subsurface reflectance and a denominator that represented the total subsurface reflectance. Any spatial variation in the illumination light I_0 was canceled when calculating Pol. The effects of any spatial variation in epidermal melanin pigmentation such as freckles or age marks were canceled. The final Pol image was insensitive to variations in illumination light intensity and variations in surface pigmentation and was sensitive to the superficially scattered polarized illumination light.

2.3 Illustrating Optical Coupling

Two subjects (Caucasian) were imaged at the Oregon Medical Laser Center, Providence St. Vincent Medical Center. One was a normal adult skin site. The second was a burn site on an adult who was burned as a youth. These images are shown in Figure 2.

2.4 Illustrating the Point Spread Function

A third subject (Caucasian) was imaged at the Oregon Medical Laser Center (same system as earlier) while casting a shadow from the edge of a razor blade onto the skin (Figure 3). The razor blade cast a sharply defined shadow on the skin. The light that entered the skin in the illuminated skin area was multiply scattered and migrated through the skin into the shaded area. Light collected as I_{par} and I_{per} from the shaded area had experienced multiple scattering events within the tissue. The Pol image was calculated and the distance to which the I_{par}, I_{per}, and Pol signals extended into the shadow provided an estimate of the point spread function for crosstalk between pixels in Pol images of skin. A white paper card was imaged to specify the position of the shadow edge as the midpoint between the maximum values and minimum values. For each image, the I_{par} and I_{per} values along a single *x*-axis line perpendicular to the edge of the shadow was acquired using MATLAB™. The average of 300 such line traces was determined. This average was plotted versus *x* to indicate the I_{par} and I_{per} behavior relative to the edge of the shadow. The Pol values versus *x* were calculated using these average I_{par} and I_{per} traces.

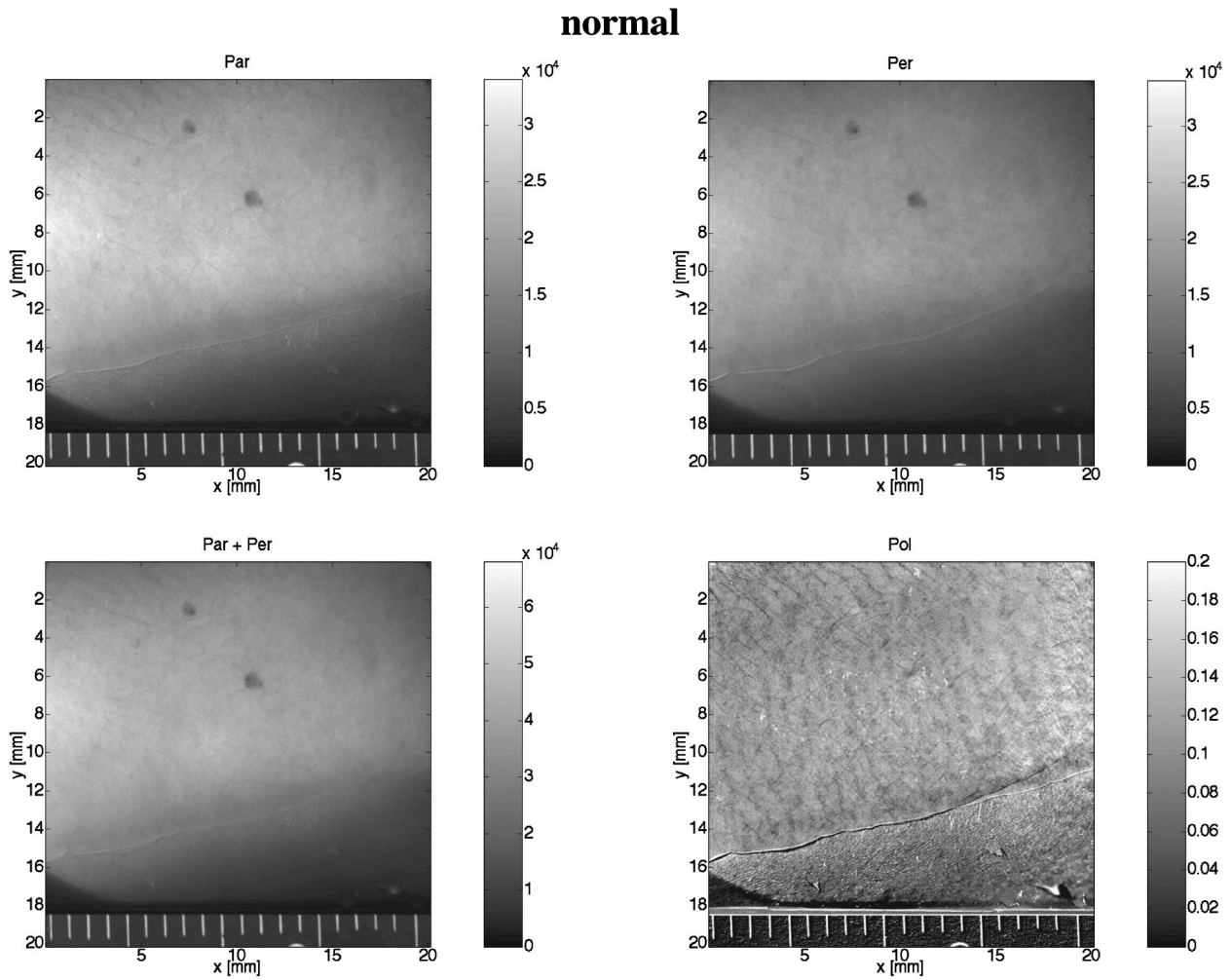

Fig. 2 Images of (left) normal skin site, and (right) skin burn scar. (a) I_{par} image. (b) I_{per} image. (c) $I_{par}+I_{per}$ image. (d) Pol image. Notice I_{par} image is slightly brighter than I_{per} image due to reflectance of incident light by superficial layers. Pol image isolates this superficial scattering and reveals the structural details of the superficial layer. Note the boundary between areas coupled and not coupled by a drop of water, illustrating the importance of water coupling of the glass plate to the skin in order to reject the glare specularly reflected from the air/tissue surface. In the normal skin site (left), notice the dermal structure revealed in the Pol image. In the burn skin site (right), notice that the burn appears whiter than normal skin in the I_{per} and I_{par} images but appears darker than normal skin in the Pol images.

2.5 Pilot Clinical Study

In a pilot clinical study of human patients [Figures 4(a)–4(o)], the color filter was omitted and the images used a full-spectrum of white light source (Dolan-Jenner Industries, Woburn, MA). Images were acquired as 435×548 images with 39×39 μm^2 pixels using IPLab™ to control the camera. Analysis used IPLab™ software.

The CCD camera was mounted on a universal joint on a balanced photographic boom arm (Red Wing) so that the camera could be positioned normal to any skin surface of a patient. Ten patients in the dermatology clinic of the Veterans' Administration Hospital, Oregon Health and Science University, who presented various skin pathologies were imaged. The camera was coupled to the skin by a drop of water. Two images were acquired in a few seconds while the skin site was held stationary against the glass plate in the image plane of the camera. Image processing was accomplished at a later time.

3 Results and Discussion

3.1 Normal Skin and Skin Burn Scar

Figure 2 shows four images each for a normal skin site and a skin burn site that was acquired by the adult subject as a youth and had undergone scarring. The four images are I_{par}, I_{per}, $I_{par}+I_{per}$, and Pol. There was a slight increase of reflected light in I_{par} relative to I_{per} due to the superficial scattering of incident polarized light. The $I_{par}+I_{per}$ was equivalent to the total reflectance that one would observe by eye. The I_{par}, I_{per}, and $(I_{par}+I_{per})$ images were all very similar. The Pol was very different and emphasized the scattering of incident polarized light by superficial tissues.

The tissue was coupled to the glass plate by a drop of water and the water-line margin between coupled and uncoupled areas is visible in the figures. The Pol image shows how the specular reflectance from the air/tissue surface dominated the image when there was no optical coupling between

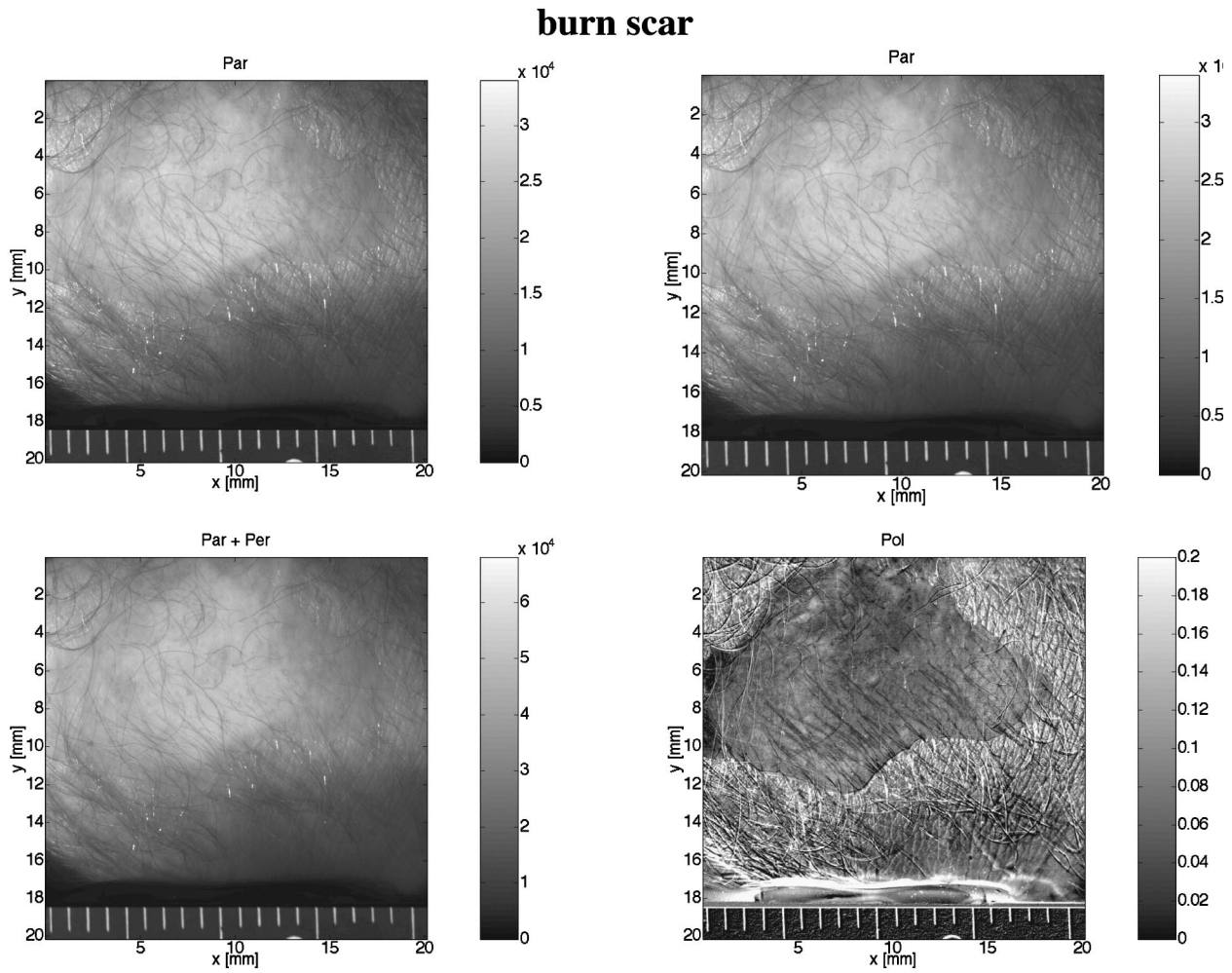

Fig. 2 (*Continued.*)

the glass plate and the skin. The skin area not coupled by water to the glass plate presented a large amount of specularly reflected light. Since the skin surface was rough, there was surface glare despite the illumination light being delivered from an angle. The signal contributed by such glare was stronger than the Pol image of interest. Without the optical coupling, the desired Pol image was masked by this surface glare signal.

Figure 2 (left) shows the images for the normal skin with two pigmented nevi. The texture of the dermis is revealed in the Pol image as striations. The pigmentation of the two superficial nevi are largely canceled in the Pol image.

Figure 2 (right) shows the images for the skin burn scar. The I_{per} and I_{par} images show the burn scar as a white region due to the strong backscatter from the collagen fibers induced by the burn trauma. However, the Pol image shows this region as a darker signal relative to normal skin. The collagen fibers in the burn scar are randomizing the polarized illumination faster than they are backscattering the polarized illumination. The balance between the rate of randomization and the rate of backscattering may be influenced by the size of collagen fiber bundles in the scar. While the I_{per} and I_{par} images show a white scar, the Pol image reveals some structure in the scar, suggesting that Pol images may prove useful in evaluating the topography of scarring.

3.2 Estimating the Point Spread Function

Figure 3 shows the experiment where a razor blade cast a shadow onto the skin surface. The experiment illustrates how light diffuses from an illuminated area into a shaded area on a forearm skin site. Figure 3(a) shows I_{par} and I_{per} as functions of position relative to the edge of the shadow. Also shown is the intensity reflected from a white paper card which identified the shadow edge. The intensities begin to fall within the illuminated area near the shadow edge due to the effect of the boundary condition on diffusion of light. Since the shadow does not contribute to light diffusion, the concentration of photons in the tissue drops in the illuminated region near the edge of the shadow.

Figure 3(b) shows the calculated Pol values as a function of position. The Pol values are about 0.08 in the illuminated area but increase significantly at positions closer to the shadow edge. The Pol values drop to zero within the shadow distant from the shadow edge. The peak of Pol at the edge drops off with a 390 μm half-width-half-max extending into

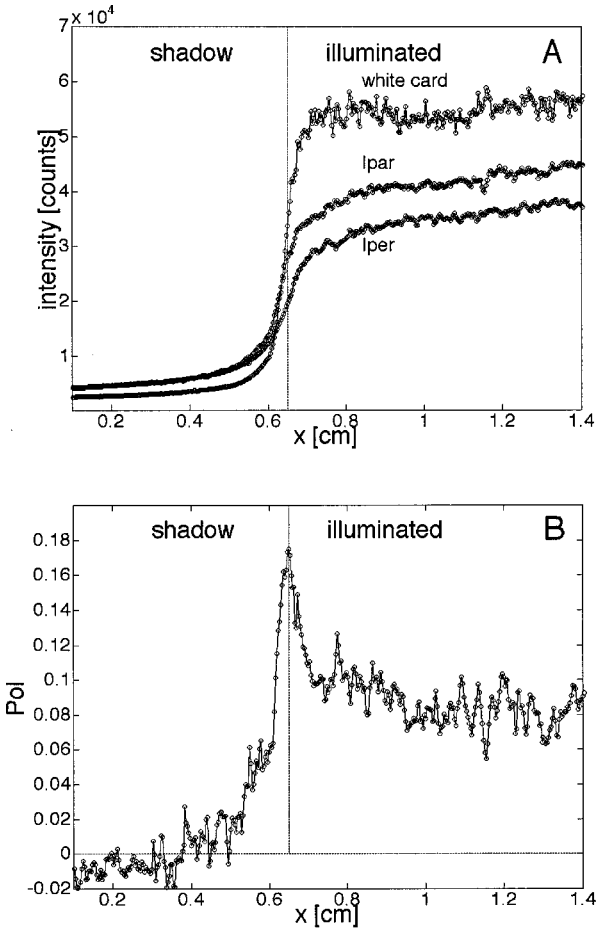

Fig. 3 Shadow of razor blade on human skin *in vivo*. (a) Average intensity as function of position, *x*, along axis perpendicular to shadow of razor blade for I_{par}, I_{per}, and intensity from a white card. (b) Pol values of skin as function of *x*. Dashed vertical line indicates edge of shadow.

the shadow and the same half-width extending into the illuminated area. The Pol values do not fall exactly to zero deep within the shadow. Far into the shadow distant from the shadow edge the I_{per} was 1.6% higher (76 counts) than the I_{par} rather than being equal as expected for light that has been randomized by diffusion. This difference was thought to be an artifact of the optical system.

The point spread function for Pol in Figure 3(b) showed a peak value near the shadow edge. Of course the deeply penetrating photons that contribute to I_{par} and I_{par} will cancel due to the subtraction in the numerator during calculation of Pol [see Eq. (2)]. Consider the role of early scattered photons from superficial layers that contribute to both I_{par} and I_{par}. Let there be two neighboring tissue sites A and B associated with camera pixels A and B, respectively. The Pol value for pixel A depends on the superficial I_{par} that reflects from tissue site A and on the superficially scattered I_{per} that has scattered from tissue site B into tissue site A and escaped from tissue site A to also contribute to pixel A. If tissue site A is at the shadow edge and tissue site B is in the shadow, there are no I_{per} photons contributed from tissue site B to tissue site A and pixel A. Therefore, pixel A at the shadow edge is depleted of superficial I_{per} photons that normally might have been scattered from tissue site B into tissue site A and escaped from tissue site A. Depletion of I_{per} photons causes the Pol value for pixel A to increase. The extent of the Pol peak into the illuminated regions characterizes this depletion of superficially scattered I_{per} photons due to the shadow. Some incident photons can also scatter into neighboring pixels and escape as I_{par} photons. The extent of the Pol peak into the shaded region characterizes this scattered contribution of superficial I_{par} photons into neighboring pixels.

3.3 Pilot Clinical Study

Figure 4 shows a series of images that compare normal light images with polarized light images. On the left of each pair of images is the normal light image, represented by I_{per}. The choice of I_{per} provides an optimal diffuse light image by avoiding specular glare. As evident in Figure 2, the I_{per} and $(I_{par}+I_{per})$ images are essentially equivalent. On the right of each pair of images is the polarized light image, Pol.

Figure 4(a) shows a ruler to specify the field of view. Figure 4(b) shows a freckle. The Pol images successfully removed the superficial epidermal pigmentation of the freckle to reveal normal skin underneath.

Figure 4(c) shows a benign pigmented nevus. The Pol image did not cancel the melanin pigmentation of the nevus but rather showed an enhanced Pol signal. One possible explanation was that the melanosomes of the nevus backscatter the incident polarized light, as they do during confocal reflectance microscopy,[22] although the superficial melanosomes of freckles did not behave this way. A second possible explanation is that when melanin pigmentation is located below the surface the melanin no longer acts as a surface filter and the cancelation of T_{mel} in Eq. (2) is incomplete and an apparent Pol signal is generated. A third possible explanation is that the nevus had structure that backscattered polarized illumination. The Pol image showed a dark area corresponding to the epidermal infolding around each hair follicle, which was not seen with normal light. A possible explanation is that the polarized illumination light is not strongly reflected by the epidermis relative to the dermis and so the Pol signal is decreased around the hair follicles. In the skin areas between hair follicles, the Pol signal is stronger and may originate from the initial backscatter from the collagen fibers of the dermis before the collagen fibers can depolarize the illumination. In the Pol figure, the texture of the dermis seems evident as if the Pol image is faithfully imaging the papillary and upper reticular dermis. Figures 4(d)–4(f) show compound pigmented nevi illustrating the variation in images that can be encountered clinically.

Figure 4(g) shows a black tattoo. The tattoo particles reflect a strong Pol signal which presents as a white coloration in the Pol image. Apparently polarized light is penetrating sufficiently deep to encounter these particles and be reflected as still polarized I_{par}. A working hypothesis is that the tattoo particles present a strong refractive index difference that causes strong backscattered reflectance of the polarized illumination light.

Figures 4(h)–4(o) are nonpigmented lesions: a nonpigmented intradermal nevus, neurofibroma, actinic keratosis, malignant basal cell carcinoma, squamous cell carcinoma, and

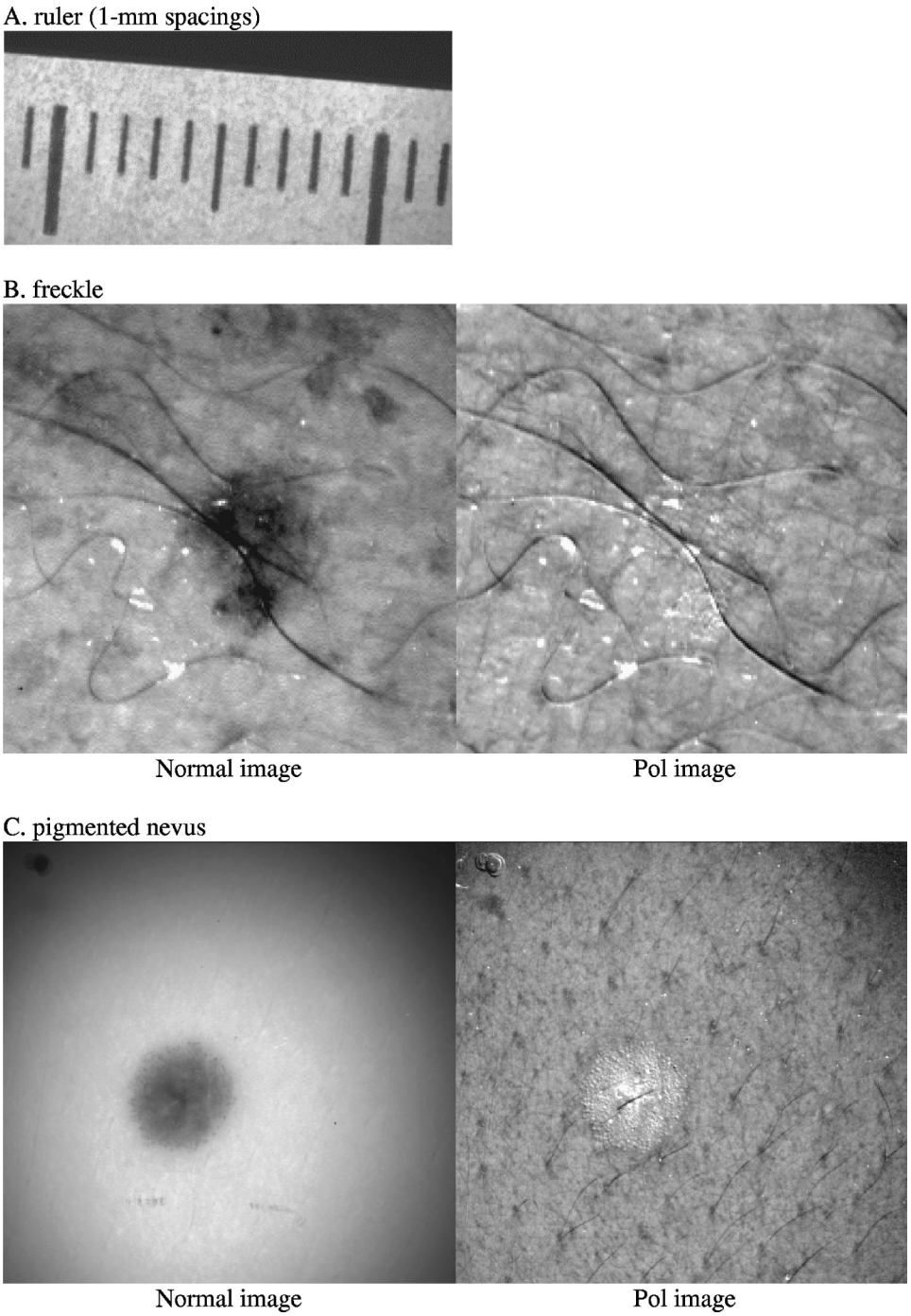

Fig. 4 Images of skin sites representing various skin pathologies. For each pair of images: (Left) normal light image represented by I_{par} image; (Right) polarized light image represented by Pol image.

vascular abnormality (venous lake). In all cases, the Pol image provides an image that captures the texture and structure of the lesion as it invades or modifies the surrounding normal skin.

During acquisition of the I_{par} and I_{per} images, any movement by the patient resulted in the misregistration of the two images. One common example is that hairs sometimes showed as a pair of black and white lines. Such misalignment was clearly evident in the tattoo of Figure 4(g). However, the skin pressed against the glass was more stationary than the hairs, especially thicker hairs that can behave like little springs and move while the underlying skin remains fixed by the surface contact with the glass plate. A new camera system, now being completed, overcomes this problem by automating the rotation of the analyzing polarizer to provide rapid image acquisition that minimizes movement artifacts.

Another common artifact in these pilot study images occurs when the water droplet used for optically coupling the skin to the glass plate captures some air bubbles and traps a glass/air/skin interface within the field of view. The air/water

D. compound nevus

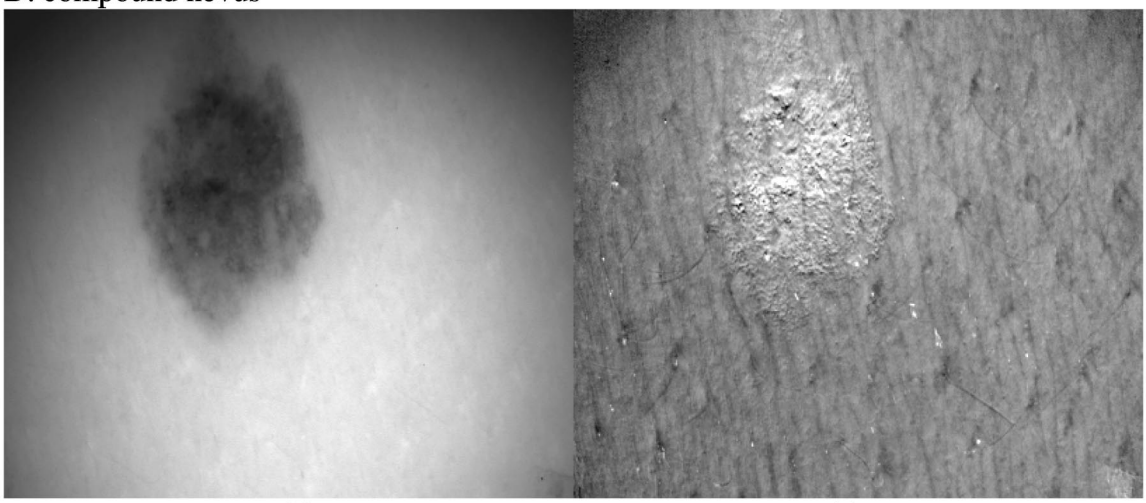

Normal image Pol image

E. compound nevus

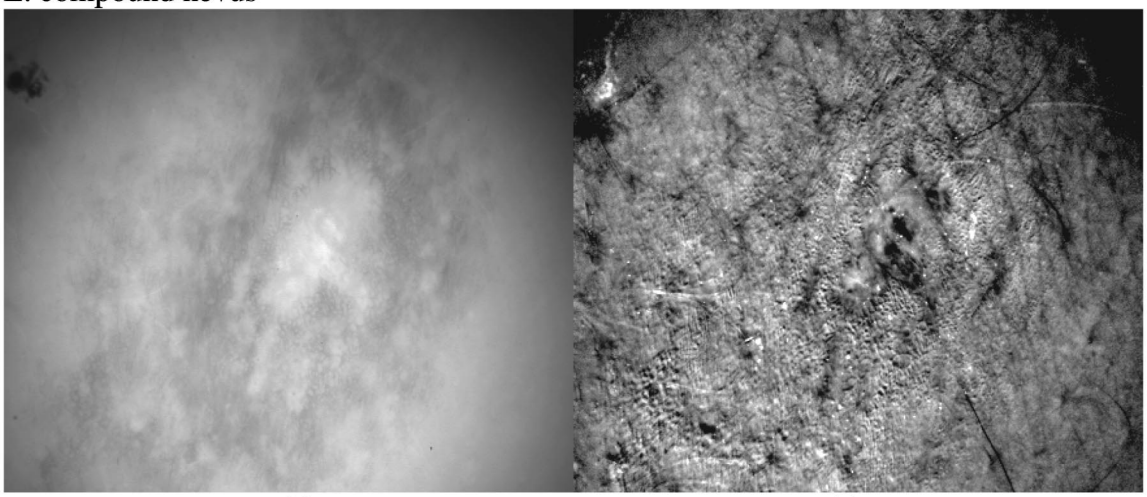

Normal image Pol image

F. compound nevus with atypical features

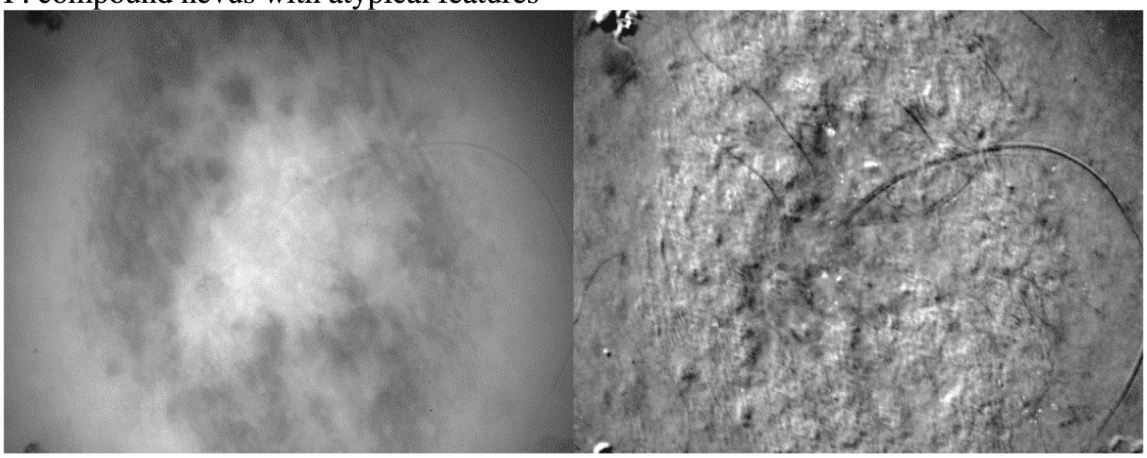

Normal image Pol image

Fig. 4 (*Continued.*)

G. black tattoo

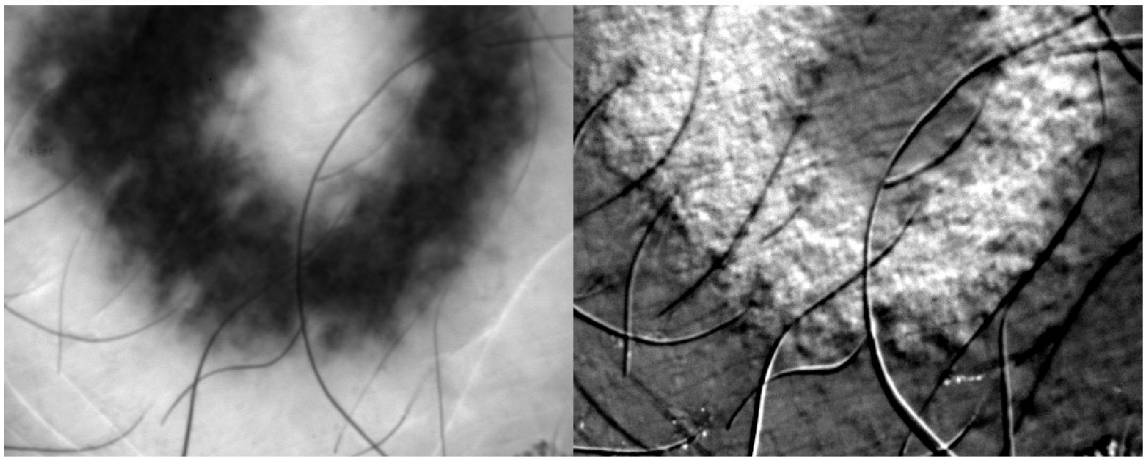

Normal image Pol image

H. nonpigmented intradermal nevus

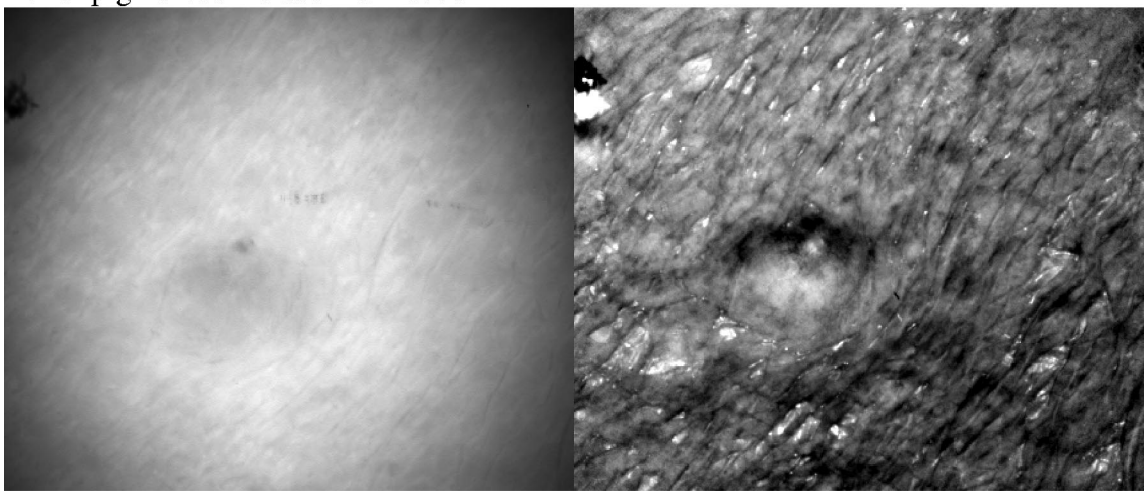

Normal image Pol image

I. neurofibroma

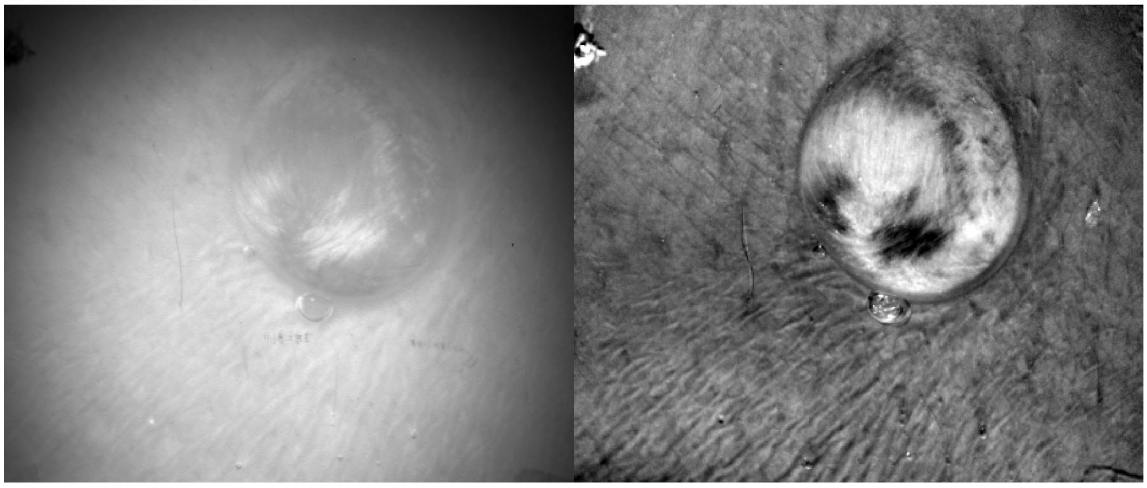

Normal image Pol image

Fig. 4 (*Continued.*)

J. actinic keratosis

K. actinic keratosis

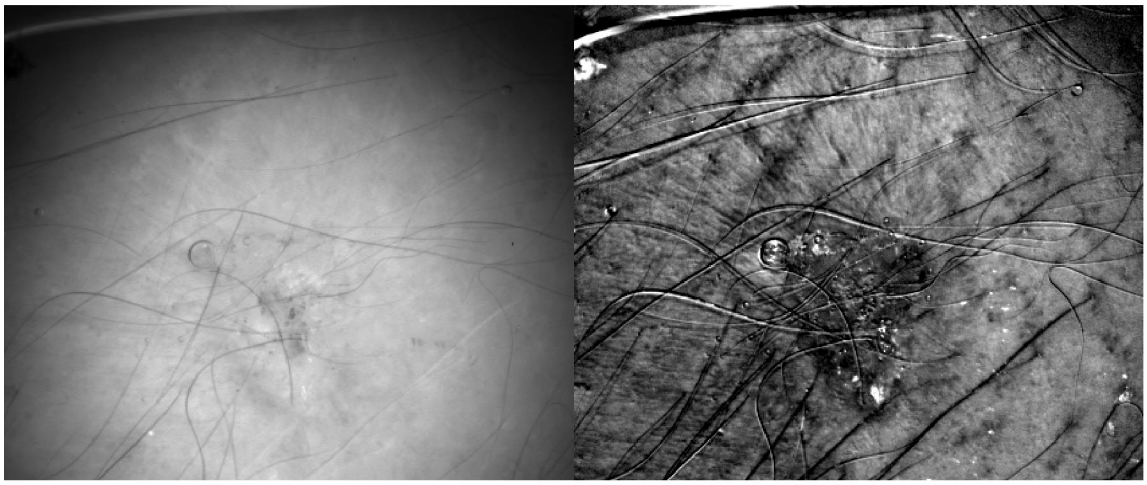

Normal image Pol image

L. malignant basal cell carcinoma

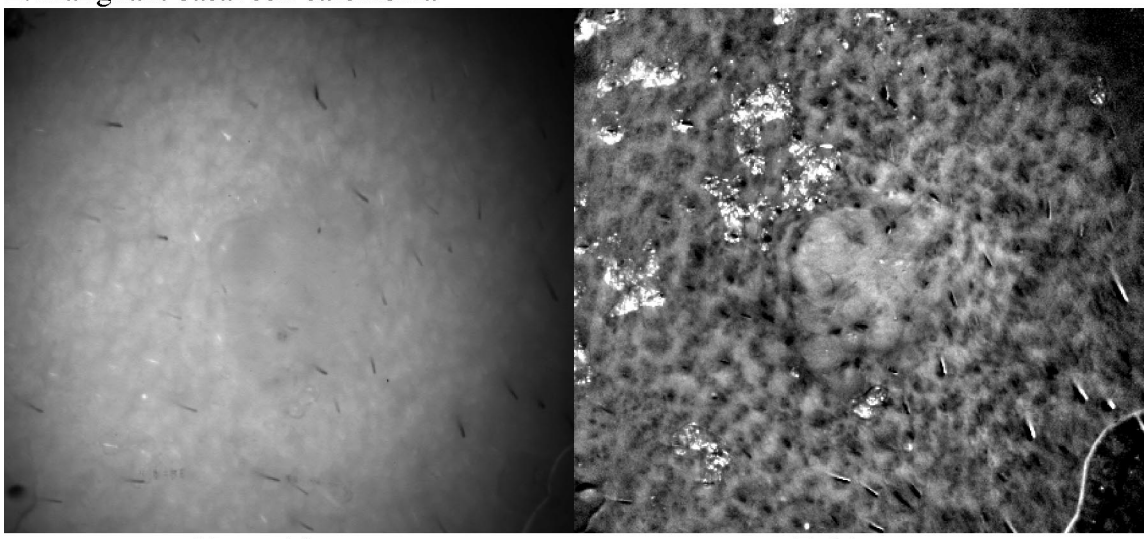

Normal image Pol image

Fig. 4 (***Continued.***)

M. malignant basal cell carcinoma

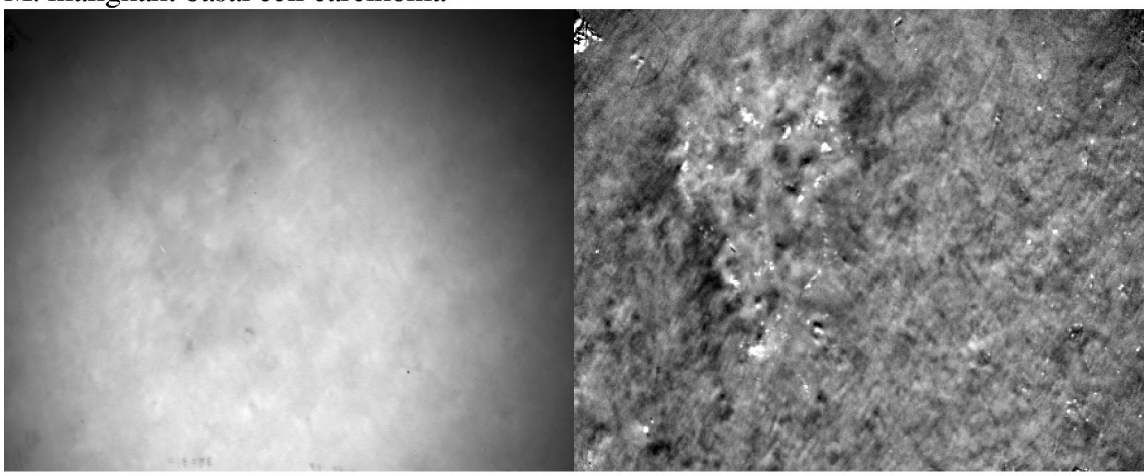

Normal image Pol image

N. squamous cell carcinoma

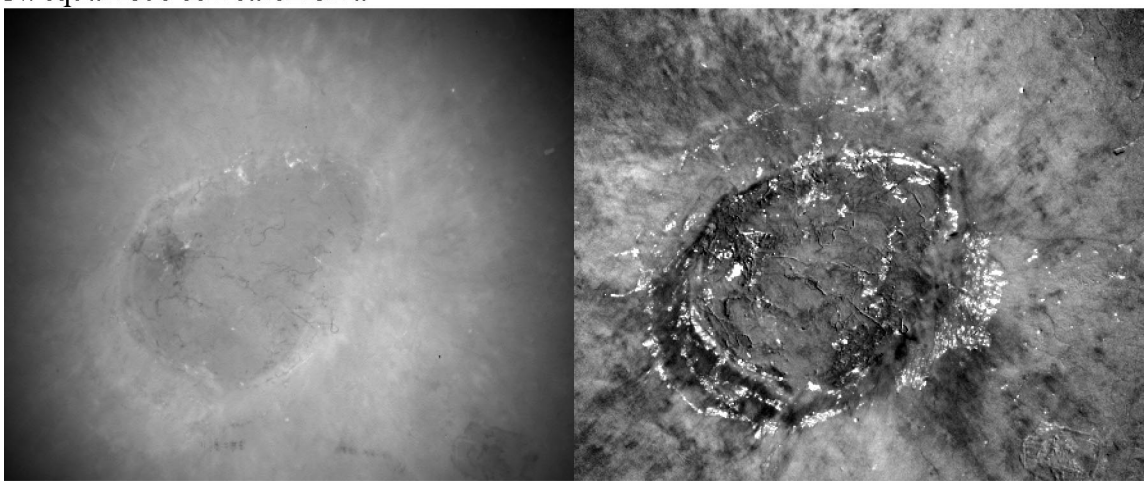

Normal image Pol image

O. vascular abnormality (venous lake)

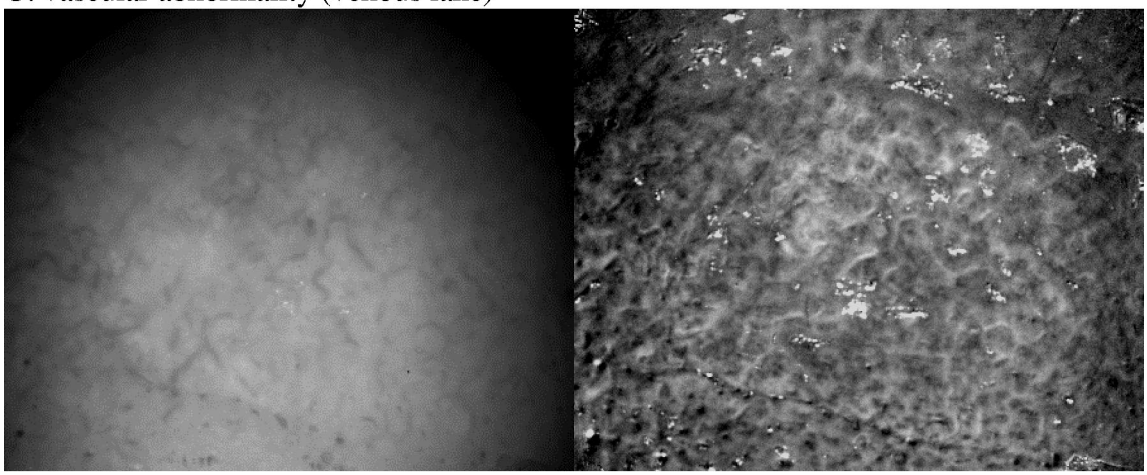

Normal image Pol image

Fig. 4 (***Continued.***)

or air/skin interfaces strongly reflect polarized illumination light yielding a high Pol value that is not representative of the tissue. For example, Figures 4(b), 4(h), 4(j), 4(l), and 4(o) all show such air bubbles which appear as bright white spots in the image. A more viscous coupling agent is needed to ensure more reliable wetting of the tissue surface and coupling to the glass plate.

4 Conclusion

In summary, the Pol image is dominated by the I_{par} photons that directly scatter from a pixel and there is less contribution due to I_{par} and I_{per} photons that scatter into the pixel of interest from neighboring pixels. The contribution of such photons scattered from neighboring pixels appears to fall to half-max at a distance of about 390 μm. The Pol images are therefore able to emphasize image contrast on the basis of light scattering in the superficial layers of the skin. The Pol images can visualize the disruption of the normal texture of the papillary and upper reticular dermis by skin pathology. This project is currently being translated into the Mohs surgery clinic where Pol images may identify skin cancer margins and guide surgical excision of skin cancer.

Acknowledgments

This work was supported by the National Institutes of Health (Contract Nos. RO1-CA80985 and RO1-CA84587).

References

1. R. R. Anderson, ''Polarized light examination and photography of the skin,'' *Arch. Dermatol.* **127**, 1000–1005 (1991).
2. J. M. Schmitt, A. H. Gandjbakhche, and R. F. Bonner, ''Use of polarized light to discriminate short-path photons in a multiply scattering medium,'' *Appl. Opt.* **32**, 6535–6546 (1992).
3. S. L. Jacques, M. R. Ostermeyer, L. Wang, and D. Stephens, ''Polarized light transmission through skin using video reflectometry: Toward optical tomography of superficial tissue layers,'' *Proc. SPIE* **2671**, 199–210 (1996).
4. M. R. Ostermeyer, D. V. Stephens, L. Wang, and S. L. Jacques, ''Nearfield polarization effects on light propagation in random media,'' in: *OSA TOPS on Biomedical Optical Spectroscopy and Diagnostics*, E. Sevick-Muraca and E. Benaron, Eds., Vol. 3, pp. 20–25, Optical Society of America, Washington, DC (1996).
5. S. G. Demos and R. R. Alfano, ''Optical polarization imaging,'' *Appl. Opt.* **36**, 150–155 (1997).
6. S. L. Jacques and K. Lee, ''Polarized video imaging of skin,'' *Proc. SPIE* **3245**, 356–362 (1998).
7. A. H. Hielscher, J. R. Mourant, and I. J. Bigio, ''Influence of particle size and concentration on the diffuse backscattering of polarized light from tissue phantoms and biological cell suspensions,'' *Appl. Opt.* **36**, 125–135 (1997).
8. J. R. Mourant, A. H. Hielscher, J. P. Freyer, T. M. Johnsom, and A. A. Eick, ''Scattering properties of biological cells,'' in *Spring Topical Meetings*, Optical Society of America, Orlando, FL (8–11 March 1998).
9. G. Jarry, E. Steimer, V. Damaschini, M. Epifanie, M. Jurczak, and R. Kaiser, ''Coherence and polarization of light propagating through scattering media and biological tissues,'' *Appl. Opt.* **37**, 7357–7367 (1998).
10. V. Sankaran, K. Schönenberger, T. Walsh, and D. J. Maitland, ''Polarization discrimination of coherently propagating light in turbid media,'' *Appl. Opt.* **38**(19), 4252–4261 (1999).
11. S. L. Jacques, R. J. Roman, and K. Lee, ''Imaging superficial tissues with polarized light,'' *Lasers Surg. Med.* **26**, 119–129 (2000).
12. V. Sankaran, M. J. Everett, D. J. Maitland, and J. T. Walsh, ''Comparison of polarized light propagation in biologic tissue and phantoms,'' *Opt. Lett.* **24**, 1044–1046 (1999).
13. V. Sankaran, J. T. Walsh, and D. J. Maitland, ''Polarized light propagation through tissue phantoms containing densely packed scatterers,'' *Opt. Lett.* **25**, 239–241 (2000).
14. R. C. Studinski and I. A. Vitkin, ''Methodology for examining polarized light interactions with tissues and tissue-like media in the exact backscattering direction,'' *J. Biomed. Opt.* **5**, 330–337 (2000).
15. C. Brosseau, *Fundamentals of Polarized Light: A Statistical Optics Approach*, Wiley, New York (1988).
16. V. Backman, R. Gurjar, K. Badizadegan, R. Dasari, I. Itzkan, L. T. Perelman, and M. S. Feld, ''Polarized light scattering spectroscopy for quantitative measurement of epithelial cellular structures *in situ*,'' *IEEE J. Sel. Top. Quantum Electron.* **5**, 1019–1027 (1999).
17. L. T. Perelman, V. Backman, M. Wallace, G. Zonios, R. Manoharan, A. Nusrat, S. Shields, M. Seiler, C. Lima, T. Hamano, I. Itzkan, J. Van Dam, J. M. Crawford, and M. S. Feld, ''Observation of periodic fine structure in reflectance from biological tissue: A new technique for measuring nuclear size distribution,'' *Phys. Rev. Lett.* **80**, 627–630 (1998).
18. K. Sokolov, R. Drezek, K. Gossage, and R. Richards-Kortum, ''Reflectance spectroscopy with polarized light: Is it sensitive to cellular and nuclear morphology,'' *Opt. Express* **5**, 302–317 (1999).
19. J. F. de Boer, T. E. Milner, M. J. C. van Gemert, and J. S. Nelson, ''Two-dimensional birefringence imaging in biological tissue by polarization-sensitive optical coherence tomography,'' *Opt. Lett.* **22**, 934–936 (1997).
20. G. Yao and L. V. Wang, ''Depth-resolved two-dimensional Stokes vectors of backscattered light and Mueller matrices of biological tissue measured with optical coherence tomography,'' *Appl. Opt.* **24**, 537–539 (1999).
21. M. H. Smith, ''Interpreting Mueller matrix images of tissues,'' *Proc. SPIE* **4257**, 82–89 (2001).
22. M. Rajadhyaksha, M. Grossman, D. Esterowitz, R. H. Webb, and R. R. Anderson, ''*In vivo* confocal scanning laser microscopy of human skin: melanin provides strong contrast,'' *J. Invest. Dermatol.* **104**, 946–952 (1995).